Annals of Biomedical Engineering (© 2016)
DOI: 10.1007/s10439-016-1694-3

Sonomicrometry-Based Analysis of Post-Myocardial Infarction Regional Mechanics

EVA ROMITO,[1,2] HEATHER DOVIAK,[2,3] CHRISTINA LOGDON,[2,3] PARKER FREELS,[2] TAREK SHAZLY,[1] and FRANCIS G. SPINALE[1,2,3,4]

[1]University of South Carolina College of Engineering and Computing, Columbia, USA; [2]Cardiovascular Translational Research Center, University of South Carolina School of Medicine, Columbia, USA; [3]Department of Cell Biology and Anatomy, University of South Carolina School of Medicine, Columbia, USA; and [4]WJB Dorn Veteran Affairs Medical Center, Columbia, SC, USA

(*Received 20 April 2016; accepted 5 July 2016*)

Associate Editor Karyn Kunzelman oversaw the review of this article.

Abstract—Following myocardial infarction (MI), detrimental changes to the geometry, composition, and mechanical properties of the left ventricle (LV) are initiated in a process generally termed adverse post-MI remodeling. Cumulatively, these changes lead to a loss of LV function and are deterministic factors in the progression to heart failure. Proposed therapeutic strategies to target aberrant LV mechanics post-MI have shown potential to stabilize LV functional indices throughout the remodeling process. The *in vivo* quantification of LV mechanics, particularly within the MI region, is therefore essential to the continued development and evaluation of strategies to interrupt the post-MI remodeling process. The present study utilizes a porcine MI model and *in vivo* sonomicrometry to characterize MI region stiffness at 14 days post-MI. Obtained results demonstrate a significant dependence of mechanical properties on location and direction within the MI region, as well as cardiac phase. While approaches for comprehensive characterization of LV mechanics post-MI still need to be improved and standardized, our findings provide insight into the issues and complexities that must be considered within the MI region itself.

Keywords—Myocardial infarction, Anisotropy, Heterogeneity, Myocardial stiffness.

INTRODUCTION

Despite significant improvements in achieving early reperfusion with an acute coronary syndrome, myocardial injury still commonly occurs, ultimately leading to myocardial infarction (MI) and progressive left ventricle (LV) remodeling.[8,49,59,74,77,78] This process, generally termed adverse post-MI remodeling, is a major contributory factor to the development and progression of heart failure (HF).[30,44,54,69] Due to increased survival rates following the initial coronary event, the number of patients that carry the post-MI burden has been steadily rising over the past three decades.[19,20] Currently, post-MI standard of care is largely relegated to symptomatic management, leaving patients vulnerable to the deleterious consequences of the post-MI remodeling process. As such, significant research efforts spanning academia and industry have been devoted to the development of effective strategies to curtail adverse post-MI remodeling and the progression to HF in this growing patient population.[31,35,40,41,46,55,65,81]

Adverse post-MI remodeling is a multi-factorial process, causing progressive changes in the geometry (MI region thinning, remote wall thickening, and LV dilation) and mechanical properties (MI region stiffness) of the myocardium.[6,7,13,14,36,47,68] Therefore, proposed strategies to interrupt post-MI remodeling are largely focused on restoring or stabilizing the mechanical behavior of the MI region. To date, various attempts to directly (*via* physical restraint or localized biomaterial injections) or indirectly (*via* local delivery of stem cells or bioactive compound/cells) modulate the mechanical behavior of the MI region have shown promising results in terms of *in vivo* indices of LV function.[15,18,31,46,58] To facilitate the continued advancement and clinical translation of these and other emergent strategies to attenuate the remodeling process, there is a clear need for high fidelity, *in vivo* measurements of LV wall mechanics that can characterize post-MI behavior throughout the cardiac cycle, within specific regions, and in defined directions.

Address correspondence to Tarek Shazly, University of South Carolina College of Engineering and Computing, Columbia, USA. Electronic mail: shazly@usc.sc.edu

Published online: 13 July 2016

Previous studies of post-MI mechanics have utilized quantitative approaches, including imaging modalities (ultrasound, MRI, *etc.*), physical techniques (implantable markers, tensile testing, sonomicrometry), or a combination of both to evaluate changes in LV wall stress, strain, and stiffness.[10,38,39,45,60,64,82,83] A majority of past studies have characterized myocardial mechanics at the chamber level and thus provide global measures of LV properties, response, and function (i.e., chamber stiffness, segmental shortening, and wall strain rate).[5,24,43,52,57,60,64,70,84,85] Continued advancements in both image-based and physical techniques have enabled increasingly precise quantification of regional mechanical behavior and thus distinction of normal and infarcted myocardial mechanics. One of the fundamental techniques used previously for the purpose of mechanical assessment in the myocardium is sonomicrometry, which allows for high fidelity measurements of defined segmental lengths in both the spatial (0.024 mm) and temporal (>1 MHz data acquisition rate) domains.[2,16,21,29,37,71,82] While sonomicrometry has been used to examine the mechanical behavior of a specific myocardial segment/direction, no studies have fully exploited this method to examine how regional mechanical properties vary with direction, location, and cardiac phase in the post-MI context.

Past studies have primarily focused upon regional systolic performance following MI and hence have examined regional mechanics at only one point in the cardiac cycle.[17,32,33,56,73] In addition, many sonomicrometry studies are performed at early post-MI time points when the infarct region is still undergoing the acute wound healing response, which can potentially confound mechanical measurements.[1,11,17,75,76,82] These limitations motivate the use of sonomicrometry in a large animal MI model to enable high fidelity mechanical measurements throughout the cardiac cycle and within a well-defined and experimentally repeatable MI region.

In the present study, we used a porcine MI model, whereby a repeatable MI region with regards to size, location, and transmurality is surgically created *via* coronary artery ligation. A six-crystal sonomicrometry array was acutely implanted within the myocardium at 14 days post-MI, with an array location and structure that facilitate quantification of MI region mechanical anisotropy and heterogeneity. Regional mechanical measurements were performed at 14 day post-MI for several reasons. First, this time point represents the conclusion of the acute inflammatory/wound healing period, and the formation of an MI region composed of extracellular matrix.[33] Second, this time point represents when the healed MI begins to undergo adverse remodeling such as thinning and expansion. At this post-MI time point, sonomicrometry measurements were obtained under varying loads to assess key indices of stiffness during both the systolic and diastolic phase. As such, these measurements help distinguish between MI-induced changes in extracellular matrix properties (passive myocardial response) and the regional loss of contractile units (active response). In addition to isochronal systolic and diastolic measurements, examination of the entire pressure–chord length loop was performed in several directions to further examine regional geometric/functional changes following MI. Our findings demonstrate that mechanical heterogeneity and anisotropy are differentially altered by post-MI remodeling and underscore the need to specify cardiac phase in the quantification of MI region mechanical behavior.

MATERIALS AND METHODS

Overview

All animals were treated and cared for in accordance with the National Institutes of Health Guide for the Care and Use of Laboratory Animals, and all protocols were approved by the University of South Carolina's Institutional Animal Care and Use Committee. We utilized an adult pig model, whereby MI is induced through permanent coronary artery ligation. Our model was previously shown to yield a fully transmural MI with reproducible size, as well as consistent progression of post-MI remodeling as indicated by classical functional indices.[15,47,58] The transmural MI was confirmed in previous studies by histology and is due to the fact that this is a complete ligation with no reperfusion.[15] In this porcine MI model, wound healing completed by 2 weeks post-MI is characterized by a relative reduction in inflammation and a significant accumulation of collagen—i.e., fibrosis within the MI region.[7] Accordingly, this time point was chosen for assessment of MI region mechanical properties, with comparison to identical measurements performed in the same region of the LV in referent non-MI controls. Using 2-dimensional targeted echocardiography followed by placement of a sonomicrometry array and LV microtransducers within the region of interest,[10,19,22] steady-state and pressure-dependent measurements of functional indices and chord length data were recorded. To generate adequate sonomicrometry data for chord stiffness calculations, LV preload was altered by transient caval occlusion. Acquired data were aggregated and processed to compute stress–strain relationships and mechanical stiffness for each chord during the systolic and diastolic phases of the cardiac cycle.

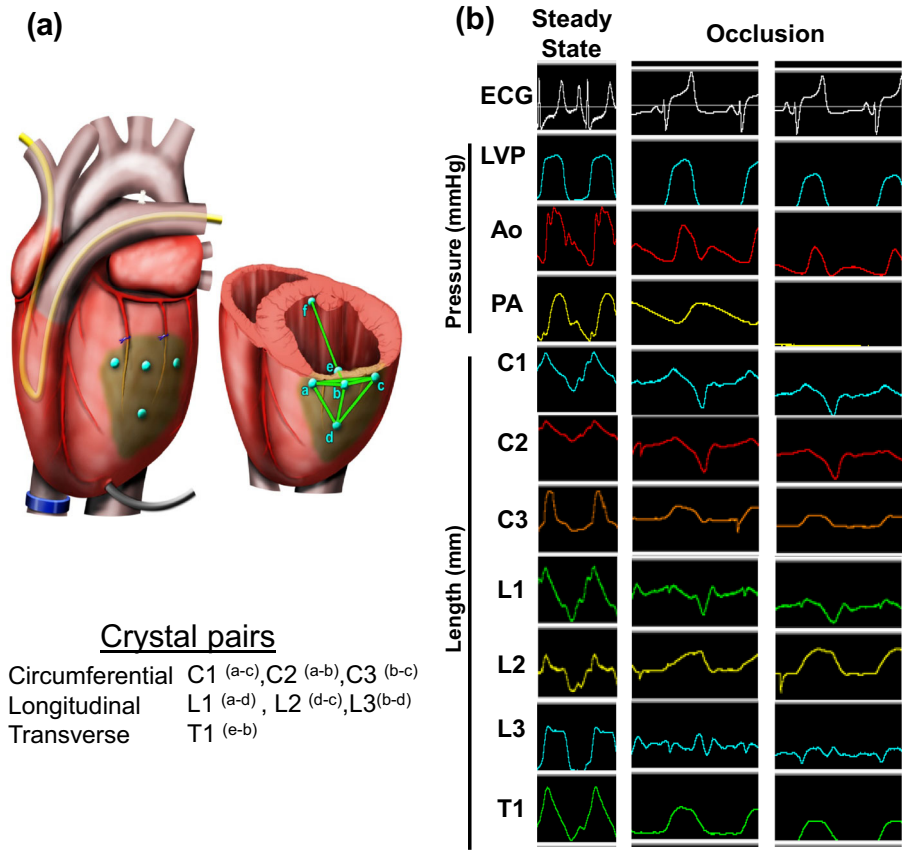

FIGURE 1. Sonomicrometry array. (a) The sonomicrometry crystal array is presented in schematic form to identify the location of the crystals and defined chords. The LV cross-sectional view demonstrates the location and relation of catheters and endocardial/epicardial crystals, whereby the small case letters identify the specific chord lengths measured. (b) Representative hemodynamic and myocardial chord lengths under steady state conditions and with transient reduction in LV pre-load by caval occlusion (LVP LV pressure, Ao Aortic pressure, PA pulmonary artery pressure).

Animal Model

A total of 11 mature male Yorkshire pigs (25 kg, Palmetto research swine, Reeseville, SC) were randomized into two different groups, a referent control ($N = 6$) and an MI group ($N = 5$). The MI group was anesthetized with isoflurane (2%) and underwent a left thoracotomy to induce MI, reproducing a previously established MI model.[47] Briefly, once access to the heart was achieved, the pericardium was opened to expose the targeted obtuse marginal arteries (OM1, OM2). These arteries were then ligated near their origin from the circumflex artery to create reproducible infarct geometry (Fig. 1a). The infarct was confirmed initially by changes in ST segment elevation in the electrocardiogram signal as well as visible blanching of the myocardium in the target MI region. Animals in the MI group were carefully monitored for the following 14 days leading to the endpoint echocardiography and sonomicrometry studies (as described below).

Ultrasound

The animals were sedated at the terminal time point with 200 mg of diazepam administered orally prior to the procedure. Two-dimensional and M-mode echocardiographic studies were then conducted from a right parasternal approach using a GE vivid 7 dimension with an M4S transducer.[15,58] Obtained measurements were processed to yield LV dimensions and functional indices.

Sonomicrometry

A custom array of six sonomicrometric crystals was implanted to monitor regional LV mechanics in both the referent control and MI groups (Sonometrics, London, Ontario, Canada). At the terminal procedure, a median sternotomy was performed and the crystal array was implanted into the LV wall at the 14 day post-MI time point for both study groups (Fig. 1a). Consistent array placement was facilitated by an

TABLE 1. Left ventricular global and regional function in referent control and post-myocardial infarction.

	Control ($N = 6$)	MI ($N = 5$)
Hemodynamics		
Heart rate (beats/min)	99 ± 4	95 ± 11
Aortic pressure (mean; mmHg)	66.6 ± 2.6	64.8 ± 4.4
End systolic pressure (mmHg)	86.8 ± 3.4	81.1 ± 4.1
d*P*/d*t* max (at 40 mm Hg; mmHg s^{-1})	1528 ± 170	1030 ± 68*
Pulmonary capillary wedge pressure (mmHg)	4.0 ± 0.1	9.1 ± 0.7*
Cardiac output (L min^{-1})	2.7 ± 0.3	1.7 ± 0.2*
End diastolic volume (mL)	50 ± 1	73 ± 3*
Diastolic posterior wall thickness (cm)	0.81 ± 0.1	0.57 ± 0.1*
Ejection fraction (%)	60 ± 1	43 ± 3*
LV sonomicrometry		
Segmental shortening (%)		
Circumferential		
C1	12.7 ± 5.9	4.8 ± 0.7
C2	14.3 ± 2.2	5.5 ± 1.3*
C3	7.1 ± 1.7	4.3 ± 1.6
Longitudinal		
L1	9.6 ± 1.6	5.9 ± 1.6*
L2	10.5 ± 2.4	9.3 ± 1.6
L3	7.6 ± 1.5	10.9 ± 1.9
Transverse		
T1†	4.8 ± 0.8	3.05 ± 0.9
LV chamber short-axis	32.5 ± 5.2	13.6 ± 2.7*
Chord stroke work (mmHg cm^{-1})		
Circumferential		
C3	3.38 ± 3.62	1.23 ± 1.21
Longitudinal		
L1	2.14 ± 2.18	3.67 ± 2.01**
Transverse		
T1	1.33 ± 1.10	0.49 ± 0.51+

Data presented as the mean ± SEM; * $p < 0.05$ vs. referent control; ** $p < 0.05$ vs. respective circumferential value; + $p < 0.05$ vs. respective longitudinal value.
Post-MI: 14 days following coronary ligation.
† Presented as wall thickening rather than segmental shortening.

implantation template (approximately a 2 cm × 2 cm grid), which spanned the MI region or analogous region in the control group. The array layout consisted of four crystals on the epicardial surface of the LV and two crystals placed subendocardially, thus producing a set of chord lengths in orthogonal directions, described as longitudinal (from base to apex), transverse (from epicardium to endocardium), and circumferential (Fig. 1a). Output from the crystal array was matched to a left ventricular pressure trace from a catheter inserted directly into the LV (Millar Instruments, Houston, TX). Changes in pressure were achieved through partial occlusion of the inferior vena cava in order to provide an effective loading range for mechanical analysis in both referent normal and MI groups (Fig. 1b). Data analysis was done on a beat-by-beat basis during steady state and occlusion runs, facilitating the quantification of pressure–chord length relationships for each chord (Ponemah software version 5.0, Data Sciences International, St. Paul, MN). Alteration of baseline loading conditions thus enabled the acquisition of sonomicrometry data at various loading conditions, which could then be processed/registered to yield stress–stretch curves that reference a specific point in the cardiac cycle (described below).

Data Analysis

Segmental Shortening

Chord lengths at end diastole and end systole were used to calculate segmental shortening. This quantity is traditionally reported as a single measure to reflect the chamber deformation along the short-axis. In the present study, segmental shortening was calculated as a percent difference in chord lengths at end diastole (EDL) and end systole (ESL), i.e., [(EDL − ESL)/EDL] × 100. Therefore, obtained data were used to quantify segmental shortening not only at the short-axis chamber level but also in orthogonal directions within the MI region.

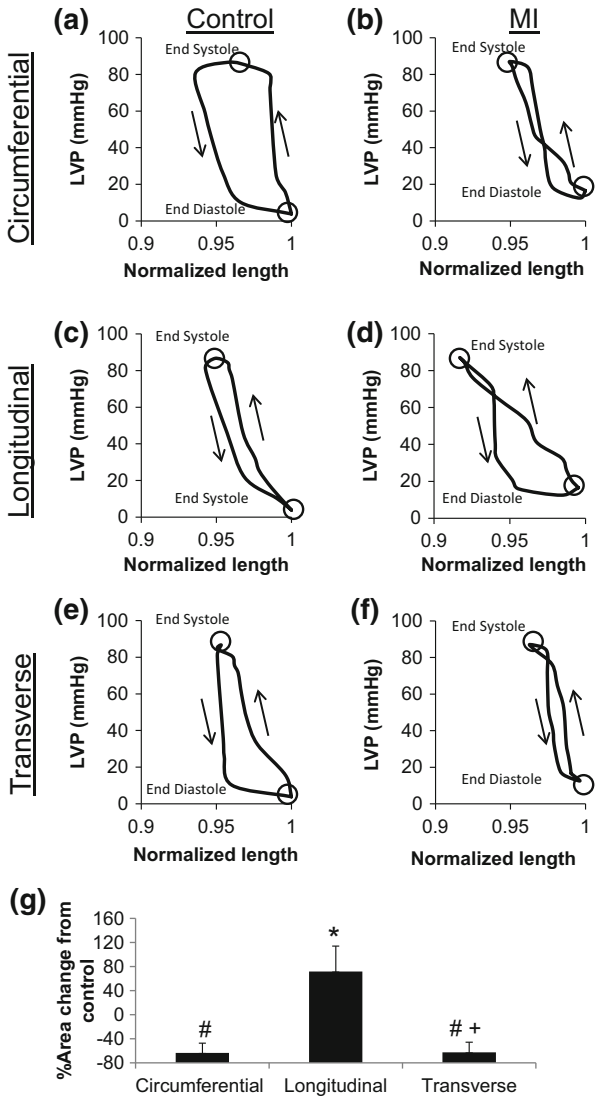

FIGURE 2. Pressure–length loops. (a–f) Sonomicrometry data from select orthogonal chords (C3, L3, and T1) were normalized and aggregated to form representative pressure–chord length loops corresponding to a full cardiac cycle. Qualitative differences in the pressure–chord length loops between referent normal and post-MI groups suggest directionally-dependence changes in the mechanical efficiency within the MI region. (g) The percent difference in the area encompassed within the pressure–length loops in the post-MI group with respect to control values in the same direction. Data shown as mean ± SEM; *$p < 0.05$ vs. circumferential value; $^{+}p < 0.05$ vs. longitudinal value; $^{\#}p < 0.05$ vs. control value (*T* test vs. 0).

Pressure–Length Loops

Chord stroke work was assessed *via* processing of pressure–chord length data obtained over a cardiac cycle. As with segmental shortening, sonomicrometry enables local quantification of chord stroke work in a manner analogous to the typical chamber-level assessment. Pressure–length loops of representative chords in each orthogonal direction were analyzed for all pigs in the control and MI groups. In order to aggregate data within each group, each chord length was normalized with respect to its maximal length throughout the cardiac cycle. The difference in areas under the loading and unloading curves in the pressure–length plane was calculated to reflect the mechanical chord work generated by contraction.

Stress–Stretch Relationships

Pressure–length curves corresponding to the systolic and diastolic phases of the cardiac cycle were generated for each chord, with pressure recorded by a catheter placed directly in the LV (Millar Instruments, Houston, TX) and chord length *via* sonomicrometry. Chord length data were further processed to yield a stretch ratio, where a theoretical initial chord length (L_0) was derived from a regression of the recorded pressure–length relationships. At each loading state, the average wall stress σ was calculated using a thin-walled spherical model for the LV, where in the circumferential and longitudinal directions

$$\sigma\ (\mathrm{g\,cm^{-2}}) = \left[\frac{PD}{4h\left(1+\frac{h}{D}\right)}\right] \times 1.36 \qquad (1)$$

where P is the chamber pressure (mmHg), D is the minor axis length (cm), h is the posterior wall thickness (cm), and 1.36 is a conversion coefficient for g cm^{-2}.[67] The pressure ranges used to calculate stress were consistent across the data sets of both study groups, with a range of 40–95 mmHg for systole and 2–10 mmHg for diastole.

Stiffness

Incremental chord stiffness was obtained *via* analysis of stress–stretch relations for each chord over the mid-range portion of pressures seen at end-systole (60–70 mmHg) and end-diastole (4–7 mmHg) during caval occlusion. Diastolic and systolic chord stiffness was calculated as the slope of the linearized stress–stretch relations over the respective pressure ranges, with registration to either end-systole or end-diastole. In the present study, these response variables are termed "systolic stiffness" and "diastolic stiffness" and are reflective of the mechanical properties within the MI region at the indicated point in the cardiac cycle.

Relative Anisotropy and Relative Heterogeneity

The relative anisotropy (RA) of mechanical stiffness within the MI region was determined using chords originating from a common crystal but oriented in each coordinate direction (circumferential, longitudi-

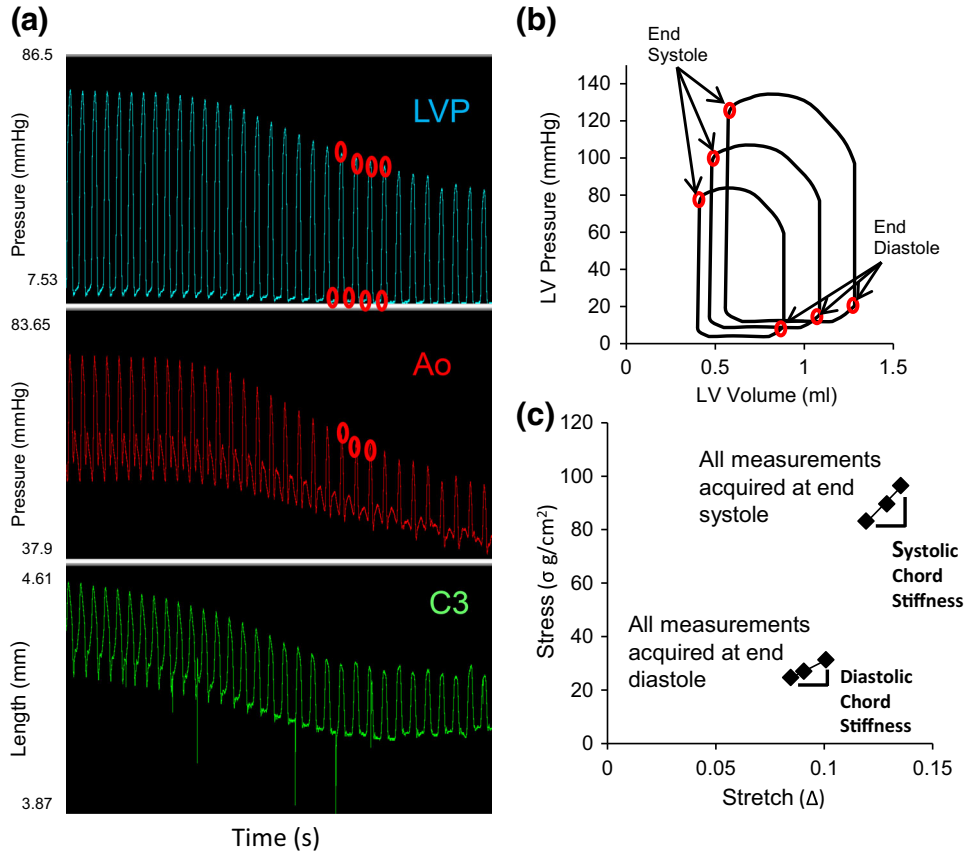

FIGURE 3. Calculation of chord stiffness (a) pressure traces [left ventricular pressure (LVP) and aortic (Ao)] and a representative (C3) crystal trace output in real time during an occlusion run. The LVP fell in a predictable manner with transient reduction in LV pre-load (top panel). The circled points on the LVP trace represent end systole and end diastole. The end systolic point was also matched to the dicrotic notch, circled on the Ao pressure trace. (b) A schematic of altered preload pressure–volume loops. The end systolic and end diastolic points are marked to represent the points where data was gathered in our occlusion runs (shown in a). (c) An illustration of chord stiffness calculations, which were based on a linearization of isochronal chord stress–stretch relations registered to either end systole or end diastole.

nal, and transverse). The RA was calculated by Eq. (2), where the stiffness of chords C1, L3, and T1 are represented by X_i, and μ represents the mean stiffness among the three chords.

$$\mathrm{RA} = \frac{1}{\mu}\sqrt{\frac{\sum_{i=1}^{3}(X_i - \mu)^2}{3}} \qquad (2)$$

The relative heterogeneity (RH) in stiffness within the MI region was determined by an analogous equation, with the three relevant chords now oriented in the same direction (circumferential) but differentially located within the MI region (chords C1–C3). The structure of the implanted crystal array was such that only the circumferential direction could be used to compute a measure of mechanical heterogeneity.

Statistical Analysis

Hemodynamic and stiffness data were analyzed using Mann–Whitney tests for significance between groups and Wilcoxon rank tests for pair-wise comparisons within groups. All other results were analyzed using non-parametric statistical tests due to the non-normal distribution of data.

RESULTS

Hemodynamics

All of the animals successfully completed the protocol, and the summary hemodynamics and global/regional indices of LV function are provided in Table 1. In the post-MI group, the maximum dP/dt values, posterior wall thickness, and ejection fraction decreased relative to control values by over ~30% ($p < 0.05$). Pulmonary capillary wedge pressure increased by 2-fold and LV end-diastolic volume increased by over 40% in the post-MI group compared to referent controls ($p < 0.05$). Thus, at 14 days following coronary occlusion, systemic hemodynamics

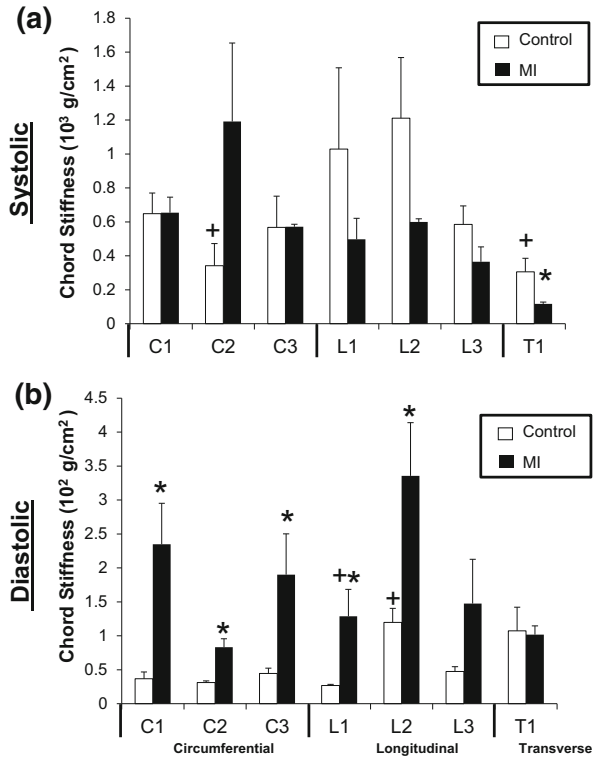

FIGURE 4. Regional stiffness. The regional stiffness modulus was computed for both the systolic and diastolic phase of the cardiac cycle by utilizing isochronal values of LV pressure and chord lengths obtained from variously loaded beats within each cardiac phase. (a) Systolic chord stiffness values exhibit chord-to-chord variation for both referent normal and MI groups, with the only statistically significant difference between the groups emerging in the transverse T1 chord. (b) Diastolic chord stiffness values exhibiting significant variation between referent normal and MI groups, with general trends reflecting an increase in chord stiffness post-MI. Data shown as mean ± SEM; *$p < 0.05$ vs. respective control values, +$p < 0.05$ vs. respective C1 chord; (note scale difference in systolic and diastolic modulus values).

and LV function/geometry were consistent with the MI phenotype, showing excellent agreement with previous studies.[15,58]

LV Sonomicrometry

Segmental Shortening

LV regional function, as measured by segmental shortening for the differently oriented chords, is shown in Table 1. In the C1 and C2 chords, segmental shortening in the post-MI group was less than half the value observed in referent controls ($p < 0.05$). Similarly, LV short axis measurements of segmental shortening obtained by sonomicrometry in the post-MI group were approximately half the value seen in referent controls ($p < 0.05$). Conversely, segmental shortening values in other directions were not significantly different between the referent control and post-MI groups, underscoring the directional dependence of this canonical functional measurement.

Pressure–Length Loops

Pressure–length relationships throughout the cardiac cycle were determined for representative orthogonal chords (C3, L3, T1) in all animals. To facilitate qualitative comparison of the directionally-dependent effects of MI, aggregate pressure–length relationships were obtained by normalizing and averaging chord length measurements within each group (Figs. 2a–2f). A notable change in the morphology of these relationships was observed between referent control and post-MI, which was particularly pronounced in the circumferential orientation. Moreover, crossover between the loading and unloading curves was observed in all directions post-MI, indicating dyskinesis within the MI region. To quantify these differences in terms of chord stroke work, the difference in areas under the loading and unloading curves in the pressure–length plane was calculated and summarized in Table 1. In the circumferential and longitudinal directions, MI induced a notable loss in the chord stroke work, with an over 50 percent reduction compared to the respective control values ($p < 0.05$, Fig. 2g). In order to more carefully examine specific regional changes in mechanics post-MI, regional stiffness during the systolic and diastolic phase with alterations in LV load was next examined.

Chord Stiffness

Chord stiffness was computed during both phases of the cardiac cycle *via* processing of isochronal values of pressure and chord length gathered during caval occlusion (Figs. 3a and 3b) to yield chord stress–stretch relations at specified points in the cardiac cycle (Fig. 3c). No consistent trend in MI-induced changes in chord stiffness was observed in systole, a finding likely reflective of active contractile units acting on the MI region and thus confounding regional mechanical property measurements (Fig. 4a). Conversely, the diastolic stiffness values for multiple chords were significantly elevated post-MI, with the most pronounced and consistent differences emerging in the circumferential direction (Fig. 4b). Specially, chords C1-C3 exhibited a 2–6 fold increase in diastolic stiffness with respect to referent controls ($p < 0.05$). In the diastolic phase, computed stiffness values are not influenced by active contraction and thus reflect the passive mechanical properties of the MI scar.

Relative Anisotropy

Most biological materials display mechanical anisotropy due to their microstructure, which can be

understood as an adaptation that promotes physiological function.[62,72] Mechanical anisotropy of the myocardium is a consequence of collagen and cardiomyocyte alignment along preferred directions, which enhances the pumping efficiency of the LV. Using our sonomicrometry array, we quantified the relative anisotropy (RA) in both control and MI groups by calculating the variance in the stiffness of chords emanating from a common point (crystal b) and oriented in the circumferential, longitudinal, and transverse directions. In the systolic phase, the MI group exhibited a significant percent increase in RA with respect to the referent control, while diastolic RA was equivalent between the groups (Fig. 5a).

Relative Heterogeneity

A localized increase in the collagen content within the MI region creates a dense, passively deforming scar.[33,50,79,80] The deposition of collagen is largely driven by the local stresses in the LV wall and is therefore a mechanobiological process with potential to alter the native mechanical heterogeneity of the myocardium.[42,48,51] Using our crystal array, we quantified the spatial dependence of circumferential chord stiffness by computing a relative heterogeneity (RH) based on the variance among chords C1–C3 (Fig. 5b). Obtained results show that the RH percent change from control was significant ($p < 0.05$) in diastole, reflecting a spatial variation in the post-MI remodeling process (Fig. 5b).

DISCUSSION

An active area of basic science as well as clinical research is to understand the basis and prevention of adverse changes in myocardial structure and function that occur following a myocardial infarction (MI), i.e., adverse post-MI remodeling. Post-MI remodeling is comprised of both regional and global changes in left ventricular (LV) geometry and composition. Together, these changes impact LV mechanics and motivate the quantification of evolving myocardial mechanical properties as a means to understand the time course and implications of heart disease progression. In particular, *in vivo* measurements of the mechanical properties of the MI region, such as stiffness, have emerged as promising targets in the development of increasingly refined therapeutic strategies to attenuate adverse post-MI remodeling.[31,34,41,61,65] In an effort to provide a comprehensive description of MI region mechanics at a critical post-MI time point, the present work utilized 2-D echocardiography and an acutely implanted sonomicrometry array to quantify MI region mechanical stiffness at 14 days post-MI in a porcine model. The sonomicrometry array structure and the inherent spatial and temporal resolution of this technique allowed for assessment of mechanical anisotropy and heterogeneity within the MI region at distinct loading conditions physiologically relevant to the systolic and diastolic phases of the cardiac cycle. The novel findings of this study include the quantification of MI region stiffness at the two ends of the cardiac cycle, as well as the assessment of how mechanical anisotropy and heterogeneity are impacted post-MI. Our findings underscore the complexity of post-MI mechanics, here manifested as directional and spatial variations in stiffness within the MI region and significant dependence on cardiac phase.

Since the area contained within a pressure–dimension relation is reflective of myocardial work, then the reduction in chord work within the MI region and in specific directions is indicative of a loss in overall mechanical performance (Fig. 2). Thus, utilizing these directional relationships in order to examine the effectiveness of emergent localized treatment strategies, such as biomaterial injections into the infarcted myocardium, would warrant consideration of this novel response variable. The use of a six crystal sonomicrometry array further allowed for the computation of seven chord stretch ratios within the MI region, which when combined with mean wall stress calculated *via* echocardiography, enabled estimation of chord stiffness. Here, the stiffness in systole was found to be less affected post-MI than its diastolic counterpart, with only one chord showing significant changes with respect to referent normal controls. The stiffness of all chords in systole was significantly higher than diastole, reflecting the influence of contraction on recorded mechanical properties and the nonlinear mechanical behavior of myocardium (even in the post-MI context).[27,28] The loss of contractile units within the MI region would suggest a decreasing systolic stiffness post-MI; however, no significant change was observed with respect to the controls. It is important to note that systolic chord stiffness computed in this study reflects local mechanical properties of the myocardium at end systole. This definition fundamentally differs from the classic response variable "end systolic myocardial stiffness", which is based on chamber-level measurements and serves as a load-independent index of contractility. This seemingly counterintuitive result can be attributed to the effect of the viable myocardium surrounding the MI, as the generated contractile forces act upon the MI region during the systolic phase of the cardiac cycle and confound explicit measurement of MI region mechanical properties. Conversely, diastolic chord stiffness was generally increased post-MI, although there was notable chord-to-chord variation in the magnitude and statistical significance of this

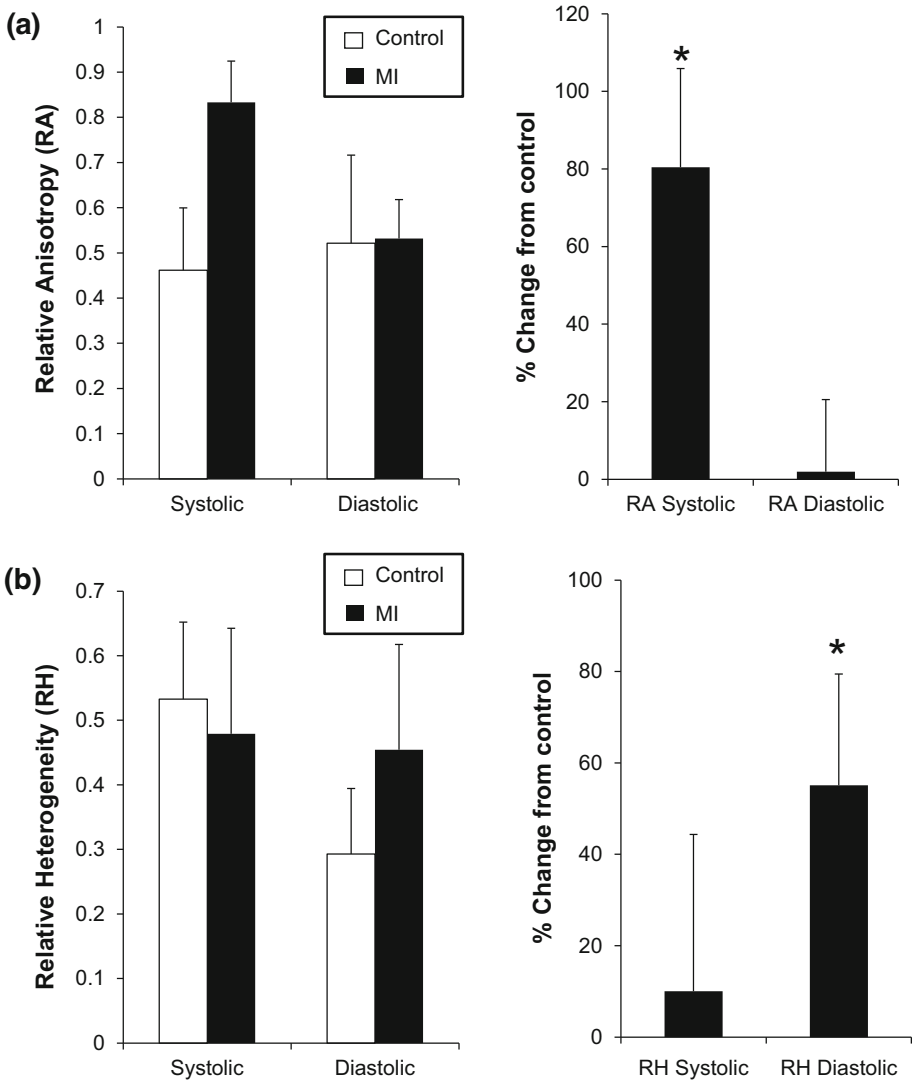

FIGURE 5. Relative anisotropy and heterogeneity. (A) The calculated relative anisotropy (RA) based on the three principal directions defined within the crystal array (circumferential, longitudinal, transverse), percent change from control RA presented adjacent. (B) Relative heterogeneity (RH) calculated from three circumferentially oriented chords in the MI region (C1, C2, C3), percent change RH presented adjacent. The percent change from control was based on a comparison of mean values of response variables obtained in the control vs. post-MI groups. Data shown as mean ± SEM; *$p < 0.05$ vs. respective control values.

change (Fig. 4). The observed increase in circumferential chord stiffness at end diastole is in agreement with a previous study by Holmes *et al.*, where a post-MI decrease in circumferential strain suggested a concomitant increase in stiffness.[25] Another study by Gupta *et al.* reported that the passive stiffness of infarcted myocardium in both circumferential and longitudinal directions increases at 1–2 weeks post-MI in sheep, although this did not correlate with collagen content.[22] Taken together, these results support the notion of restoring referent normal biomechanical properties with focus on the diastolic cardiac phase as a promising post-MI therapeutic target.

The relative anisotropy (RA) in chord stiffness indicates the directional dependence of material properties under physiologic loading (Fig. 6, left). Normal myocardium has heavily ordered fiber architecture and as a result is mechanically anisotropic, which like many soft tissues is an evolved characteristic that promotes its biomechanical function.[9,53,62,83] Mechanical anisotropy of the normal and infarcted myocardium has been previously reported in terms of strain,[2,4,23,25,26,66] but here uniquely presented as a function of mechanical stiffness in three coordinate directions defined by the implanted sonomicrometry crystal array (circumferential, longitudinal, and transverse). The significant increase in systolic RA post-MI reflects the cumulative effects of altered material properties and geometry of the MI region as well as the active contractile forces transmitted to the MI region. Conversely, MI-induced

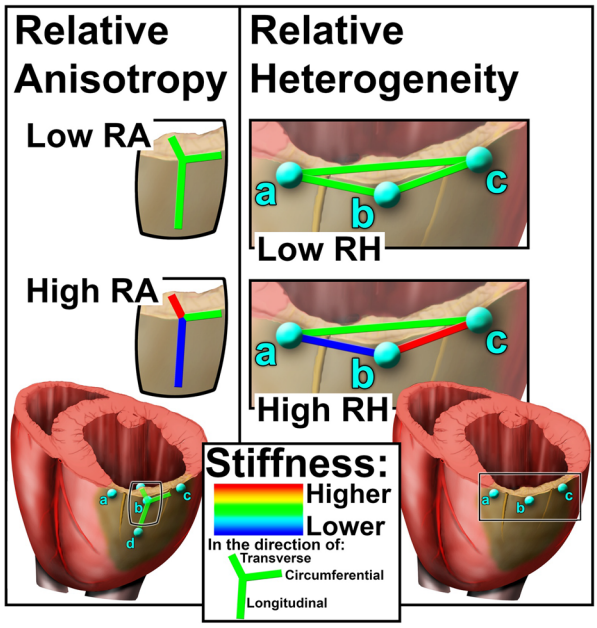

FIGURE 6. Stylized relative anisotropy and heterogeneity. The relative anisotropy (RA) quantifies the directional dependence of mechanical properties within the myocardium, here calculated as the variance in stiffness among orthogonal chords emanating from a common point in the crystal array. Relative heterogeneity (RH) quantifies the spatial dependence of mechanical properties, herein analyzed in terms of the variance of circumferentially-oriented chords with different locations/dimensions within the crystal array.

changes in diastolic RA were not significant at the 14 day post-MI time point. This finding suggests that despite the occurrence of significant adverse remodeling as indicated by hemodynamic indices, the normal extracellular matrix architecture is at least partially preserved at this post-MI time point. This finding is in qualitative agreement with previous work by Zimmerman *et al.,* where it was reported that the native microstructure of the myocardial extra cellular matrix is retained within the MI region (determined by strain and histological analysis) and serves as a scaffold that guides new collagen deposition.[86] Gupta *et al.* also noted that referent normal anisotropy in the ovine infarct is preserved up to 2 weeks post-MI, which corroborates our findings and supports the notion that native scaffold architecture guides the deposition of collagen at early times post-MI.[22]

The relative heterogeneity (RH) provides a description of the spatial variation in chord stiffness within the MI region, with our crystal array structure facilitating comparison among three circumferentially-oriented chords (Fig. 6, right). A significant increase in diastolic RH post-MI suggests that the degree of collagen synthesis and deposition differ throughout the MI region. Although the diastolic RA results discussed above suggest some retention of normal collagen architecture post-MI, the non-uniform geometry of the MI region would give rise to wall stress field heterogeneity and in turn differential rates of mechanically-mediated collagen synthesis/deposition.[3,6,12,59,63]

Limitations

Several study limitations must be considered for careful interpretation of the obtained results. Firstly, a *global* mean wall stress was used to develop chord stress–stain relationships and ultimately calculate chord stiffness, although *local* stress elevations, particularly along the border of the MI region, are likely present. A second study limitation is that post-MI mechanics were assessed at only one select post-MI time point. Although this is an acceptable time point to evaluate the effects of remodeling following significant collagen deposition in a porcine model,[32] it does not allow for full characterization of the transient mechanical changes during post-MI remodeling. Moreover, loading conditions and thus the obtained regional mechanical measurements can potentially be affected by both the opening the pericardium and the administration of anesthesia. Additionally, our findings are based upon study of posterolateral infarcts, whereas differently located MI regions may exhibit different behavior. Finally, some animal-specific variation in the shape of the MI region may occur in our MI model, which inevitably affects the placement/regional containment of the crystal array and potentially changes the sensitivity and error of obtained measurements.

Future Directions

In order to address the limitations in this study, the method by which wall stress is calculated should be improved. Specifically, our future studies will use LV geometries extracted from MRI in combination with a finite element method to solve for myocardial stress fields under prescribed loading conditions. Using this approach, more accurate chord stress–strain relationships can be developed throughout the MI region and over the cardiac cycle. The present study was limited to an analysis of regional mechanics at a single post-MI time point (14 days post-MI); future work will entail chronic studies which span the distinct phases of post-MI remodeling and will include registration of local and global mechanical response variables. An ultimate goal of this study is to improve the development and evaluation of therapeutic strategies to attenuate adverse post-MI remodeling; therefore an important future direction will be to integrate our study of local MI mechanics with specific local interventions, such as the use of injectable biomaterials to favorably alter MI

region mechanics throughout the remodeling process. Sonomicrometry, as well as other methods for *in vivo* mechanical analysis, will elucidate the mechanism by which these interventions curtail adverse post-MI remodeling and thus facilitate their clinical translation.

CONCLUSION

The use of *in vivo* sonomicrometry to characterize post-MI LV mechanics reveals a complex dependence of mechanical stiffness on the location and direction of measurements within a well-defined MI region, as well as significant variation with respect to the cardiac phase. We demonstrate that at the 14 day post-MI time point in a porcine model, the degree of mechanical heterogeneity in diastole and mechanical anisotropy in systole are significantly elevated as compared to referent normal myocardium. Efforts to comprehensively characterize transient changes of regional post-MI mechanics still need be improved; however, this work is put forth to provide insight into the complexities within the MI region itself.

ACKNOWLEDGMENTS

Figure 1 was generated by Dr. Adam Hartstone-Rose in the Department of Cell Biology and Anatomy at the University of South Carolina School of Medicine. This work was supported by the National Institute of Health grants HL11090, HL089944, HL43617, HL67922, and Merit Award from the Veterans' Affairs Health Administration. The authors wish to express their sincere appreciation to Ashley Sapp for her editorial assistance.

REFERENCES

[1]Akaishi, M., W. S. Weintraub, R. M. Schneider, L. W. Klein, J. B. Agarwal, and R. H. Helfant. Analysis of systolic bulging. Mechanical characteristics of acutely ischemic myocardium in the conscious dog. *Circ. Res.* 58:209–217, 1986.

[2]Amundsen, B. H., T. Helle-Valle, T. Edvardsen, H. Torp, J. Crosby, E. Lyseggen, A. Støylen, H. Ihlen, J. A. C. Lima, O. A. Smiseth, and S. A. Slørdahl. Noninvasive myocardial strain measurement by speckle tracking echocardiography: validation against sonomicrometry and tagged magnetic resonance imaging. *J. Am. Coll. Cardiol.* 47:789–793, 2006.

[3]Andreu, I., T. Luque, A. Sancho, B. Pelacho, O. Iglesias-García, E. Melo, R. Farré, F. Prósper, M. R. Elizalde, and D. Navajas. Heterogeneous micromechanical properties of the extracellular matrix in healthy and infarcted hearts. *Acta Biomater.* 10:3235–3242, 2014.

[4]Bachner-Hinenzon, N., O. Ertracht, A. Malka, M. Leitman, Z. Vered, O. Binah, and D. Adam. Layer-specific strain analysis: investigation of regional deformations in a rat model of acute versus chronic myocardial infarction. *Am. J. Physiol. Heart Circ. Physiol.* 303:H549–H558, 2012.

[5]Bhan, A., A. Sirker, J. Zhang, A. Protti, N. Catibog, W. Driver, R. Botnar, M. J. Monaghan, and A. M. Shah. High-frequency speckle tracking echocardiography in the assessment of left ventricular function and remodeling after murine myocardial infarction. *Am. J. Physiol. Heart Circ. Physiol.* 306:H1371–H1383, 2014.

[6]Capasso, J. M., P. Li, X. Zhang, and P. Anversa. Heterogeneity of ventricular remodeling myocardial infarction in rats after acute. *Am. J. Physiol. Hear. Circ. Physiol.* 262:H486–H495, 1992.

[7]Cleutjens, J. P., M. J. Verluyten, J. F. Smiths, and M. J. Daemen. Collagen remodeling after myocardial infarction in the rat heart. *Am. J. Pathol.* 147:325–338, 1995.

[8]Cohn, J. N., R. Ferrari, N. Sharpe, and I. Forum. Cardiac remodeling—concepts and clinical implications: a consensus paper from an international forum on cardiac remodeling. *J. Am. Coll. Cardiol.* 35(3):569–582, 2000.

[9]Demer, L. L., and F. C. P. Yin. Passive biaxial mechanical properties of isolated canine myocardium. *J. Physiol.* 339:615–630, 1983.

[10]Dhooge, J., A. Heimdal, F. Jamal, T. Kukulski, B. Bijnens, F. Rademakers, L. Hatle, P. Suetens, and G. R. Sutherland. Regional strain and strain rate measurements by cardiac ultrasound: principles, implementation and limitations. *Eur. J. Echocardiogr.* 1:154–170, 2000.

[11]Dione, D., P. Shi, W. Smith, P. Deman, J. Soares, J. Duncan, and A. Sinusas. Three-Dimensional Regional Left Ventricular Deformation from Digital Sonomicrometry. In *19th International Conference IEEE/EMBS*, pp. 848–851, 1999.

[12]Dobaczewski, M., M. Bujak, P. Zymek, G. Ren, M. L. Entman, and N. G. Frangogiannis. Extracellular matrix remodeling in canine and mouse myocardial infarcts. *Cell Tissue Res.* 324:475–488, 2006.

[13]Dobaczewski, M., C. Gonzalez-Quesada, and N. G. Frangogiannis. The extracellular matrix as a modulator of the inflammatory and reparative response following myocardial infarction. *J. Mol. Cell. Cardiol.* 48:504–511, 2010.

[14]Eaton, L. W., J. L. Weiss, B. H. Bulkley, J. B. Garrison, and M. L. Weisfeldt. Regional Cardiac Dilatation after Acute Myocardial Infarction—NEJM, 1979. http://www.nejm.org/doi/pdf/10.1056/NEJM197901113000202.

[15]Eckhouse, S. R., B. P. Purcell, J. R. McGarvey, D. Lobb, C. B. Logdon, H. Doviak, J. W. O'Neill, J. A. Shuman, C. P. Novack, K. N. Zellars, S. Pettaway, R. A. Black, A. Khakoo, T. Lee, R. Mukherjee, J. H. Gorman, R. C. Gorman, J. A. Burdick, and F. G. Spinale. Local hydrogel release of recombinant TIMP-3 attenuates adverse left ventricular remodeling after experimental myocardial infarction. *Sci. Transl. Med.* 6(223):223ra21, 2014.

[16]Fomovsky, G. M., and J. W. Holmes. Evolution of scar structure, mechanics, and ventricular function after myocardial infarction in the rat. *Am. J. Physiol. Heart Circ. Physiol.* 298:H221–H228, 2010.

[17]Fomovsky, G. M., A. D. Rouillard, and J. W. Holmes. Regional mechanics determine collagen fiber structure in

healing myocardial infarcts. *J. Mol. Cell. Cardiol.* 52:1083–1090, 2012.
[18]Fujimoto, K. L., Z. Ma, D. M. Nelson, R. Hashizume, J. Guan, K. Tobita, and W. R. Wagner. Biomaterials Synthesis, characterization and therapeutic efficacy of a biodegradable, thermoresponsive hydrogel designed for application in chronic infarcted myocardium. *Biomaterials* 30:4357–4368, 2009.
[19]Go, A. S., *et al.* Heart disease and stroke statistics–2013 update: a report from the American Heart Association. *Circulation* 127:e6–e245, 2013.
[20]Go, A. S., *et al.* Heart disease and stroke statistics–2014 update: a report from the American Heart Association. *Circulation* 129:e28–e292, 2014.
[21]Gorman, J. H., K. B. Gupta, J. T. Streicher, R. C. Gorman, B. M. Jackson, M. B. Ratcliffe, D. K. Bogen, and L. H. Edmunds. Dynamic three-dimensional imaging of the mitral valve and left ventricle by rapid sonomicrometry array localization. *J. Thorac. Cardiovasc. Surg.* 112:712–726, 1996.
[22]Gupta, K. B., M. B. Ratcliffe, M. A. Fallert, L. H. Edmunds, and D. K. Bogen. Changes in passive mechanical stiffness of myocardial tissue with aneurysm formation. *Circulation* 89:2315–2326, 1994.
[23]Helle-valle, T., E. W. Remme, E. Lyseggen, E. Pettersen, T. Vartdal, A. Opdahl, H. Smith, N. F. Osman, H. Ihlen, T. Edvardsen, and O. A. Smiseth. Clinical assessment of left ventricular rotation and strain: a novel approach for quantification of function in infarcted myocardium and its border zones. *Am. J. Physiol. Heart Circ. Physiol.* 297(1):H257–H267, 2009. doi:10.1152/ajpheart.01116.2008.
[24]Holmes, J. W., T. K. Borg, and J. W. Covell. Structure and mechanics of healing myocardial infarcts. *Annu. Rev. Biomed. Eng.* 7:223–253, 2005.
[25]Holmes, J. W., J. A. Nunez, and J. W. Covell. Functional implications of myocardial scar structure. *Am. J. Physiol. Heart Circ. Physiol.* 272:H2123–H2130, 1997.
[26]Holmes, J. W., H. Yamashita, L. K. Waldman, and J. W. Covell. Scar remodeling and transmural deformation after infarction in the pig. *Circulation* 90:411–420, 1994.
[27]Holzapfel, G. A., and R. W. Ogden. Constitutive modelling of passive myocardium: a structurally based framework for material characterization. *Philos. Trans. A. Math. Phys. Eng. Sci.* 367:3445–3475, 2009.
[28]Humphrey, J. D. Continuum biomechanics of soft biological tissues. *Proc. R. Soc. Lond. A* 459:3–46, 2003.
[29]Jackson, B. M., J. H. Gorman, III, S. L. Moainie, T. S. Guy, N. Narula, J. Narula, M. G. S. John-Sutton, L. H. Edmunds, Jr, and R. C. Gorman. Extension of borderzone myocardium in postinfarction dilated cardiomyopathy. *J. Am. Coll. Cardiol.* 40(6):1160–1167, 2002.
[30]Jugdutt, B. I. Prevention of ventricular remodeling after myocardial infarction and in congestive heart failure. *Heart Fail. Rev.* 1:115–129, 1996.
[31]Jugdutt, B. I. Remodeling of the myocardium and potential targets in the collagen degradation and synthesis pathways. *Curr. Drug Targets Cardiovasc. Haematol. Disord.* 3(1):1–30, 2003.
[32]Jugdutt, B. I. Cyclooxygenase inhibition and adverse remodeling during healing after myocardial infarction. *Circulation* 115:288–291, 2007.
[33]Jugdutt, B. I., M. J. Joljart, and M. I. Khan. Rate of collagen deposition during healing and ventricular remodeling after myocardial infarction in rat and dog models. *Circulation* 94:94–101, 1996.
[34]Kellar, R. S., B. R. Shepherd, D. F. Larson, G. K. Naughton, and S. K. Williams. Cardiac patch constructed from human fibroblasts attenuates reduction in cardiac function after acute infarct. *Tissue Eng.* 11:1678–1687, 2005.
[35]Kelley, S. T., R. Malekan, J. H. Gorman, III, B. M. Jackson, C. Robert, Y. Suzuki, T. Plappert, D. K. Bogen, M. G. Sutton, and L. H. Edmunds, Jr. Restraining infarct expansion preserves left ventricular geometry and function after acute anteroapical infarction. *Circulation* 99:135–142, 1999.
[36]Klepach, D., L. C. Lee, J. F. Wenk, M. B. Ratcliffe, T. I. Zohdi, J. A. Navia, G. S. Kassab, E. Kuhl, and J. M. Guccione. Growth and remodeling of the left ventricle: a case study of myocardial infarction and surgical ventricular restoration. *Mech. Res. Commun.* 42:134–141, 2012.
[37]Korinek, J., J. Vitek, P. P. Sengupta, A. Romero-Corral, V. K. Krishnamoorthy, E. M. McMahon, B. K. Khandheria, and M. Belohlavek. Does implantation of sonomicrometry crystals alter regional cardiac muscle function? *J. Am. Soc. Echocardiogr.* 20:1407–1412, 2007.
[38]Korinek, J., J. Wang, P. P. Sengupta, C. Miyazaki, J. Kjaergaard, E. McMahon, T. P. Abraham, and M. Belohlavek. Two-dimensional strain—a Doppler-independent ultrasound method for quantitation of regional deformation: validation in vitro and in vivo. *J. Am. Soc. Echocardiogr.* 18:1247–1253, 2005.
[39]Kraitchman, D. L., A. A. Young, D. C. Bloomgarden, Z. A. Fayad, L. Dougherty, V. A. Ferrari, R. C. Boston, and L. Axel. Integrated MRI assessment of regional function and perfusion in canine myocardial infarction. *Magn. Reson. Med.* 40:311–326, 1998.
[40]Leor, J., S. Aboulafia-Etzion, A. Dar, L. Shapiro, I. M. Barbash, A. Battler, Y. Granot, and S. Cohen. Bioengineering cardiac grafts: a new approach to repair the infarcted myocardium? *Circulation* 102(19 Suppl 3):III56–III61, 2000. doi:10.1161/01.CIR.102.suppl.
[41]Leor, J., and S. Cohen. Myocardial tissue engineering: creating a muscle patch for a wounded heart. *Ann. N.Y. Acad. Sci.* 1015:312–319, 2004.
[42]MacKenna, D., S. R. Summerour, and F. J. Villarreal. Role of mechanical factors in modulating cardiac fibroblast function and extracellular matrix synthesis. *Cardiovasc. Res.* 46:257–263, 2000.
[43]Marinkovid, J., J. Lee, M. Tan, and J. D. Thomas. Serial assessment of left ventricular chamber stiffness after acute myocardial infarction. *Am. J. Cardiol.* 77:361–364, 1995.
[44]McKay, R. G., M. A. Pfeffer, R. C. Pasternak, J. E. Markis, P. C. Come, S. Nakao, J. D. Alderman, J. J. Ferguson, R. D. Safian, and W. Grossman. Left ventricular remodeling after myocardial infarction: a corollary to infarct expansion. *Circulation* 74:693–702, 1986.
[45]Mojsejenko, D., J. R. McGarvey, S. M. Dorsey, J. H. Gorman, III, J. A. Burdick, J. J. Pilla, R. C. Gorman, and J. F. Wenk. Estimating passive mechanical properties in a myocardial infarction using MRI and finite element simulations. *Biomech. Model. Mechanobiol.* 14(3):633–647, 2014.
[46]Morita, M., C. E. Eckert, K. Matsuzaki, M. Noma, L. P. Ryan, J. A. Burdick, B. M. Jackson, J. H. Gorman, III, M. S. Sacks, and R. C. Gorman. Modification of infarct material properties limits. *Ann. Thorac. Surg.* 92:617–624, 2011.
[47]Mukherjee, R., T. A. Brinsa, K. B. Dowdy, A. A. Scott, J. M. Baskin, A. M. Deschamps, A. S. Lowry, G. P. Escobar,

D. G. Lucas, W. M. Yarbrough, M. R. Zile, and F. G. Spinale. Myocardial infarct expansion and matrix metalloproteinase inhibition. *Circulation* 107:618–625, 2003.

[48]Neidlinger-Wilke, C., E. S. Grood, J. H. C. Wang, R. A. Brand, and L. Claes. Cell alignment is induced by cyclic changes in cell length: studies of cells grown in cyclically stretched substrates. *J. Orthop. Res.* 19:286–293, 2001.

[49]Olivetti, G., J. M. Capasso, L. G. Meggs, E. H. Sonnenblick, and P. Anversa. Cellular basis of chronic ventricular remodeling after myocardial infarction in rats. *Circ. Res.* 68:856–869, 1991.

[50]Omens, J. H., T. R. Miller, and J. W. Covell. Relationship between passive tissue strain and collagen uncoiling during healing of infarcted myocardium. *Cardiovasc. Res.* 33:351–358, 1997.

[51]Pang, Y., X. Wang, D. Lee, and H. P. Greisler. Dynamic quantitative visualization of single cell alignment and migration and matrix remodeling in 3-D collagen hydrogels under mechanical force. *Biomaterials* 32:3776–3783, 2011.

[52]Park, T., S. F. Nagueh, D. S. Khoury, H. A. Kopelen, S. Akrivakis, K. Nasser, G. Ren, N. G. Frangogiannis, and A. Helen. Impact of myocardial structure and function postinfarction on diastolic strain measurements: implications for assessment of myocardial viability. *Am. J. Physiol. Heart Circ. Physiol.* 77030:724–731, 2006.

[53]Périé, D., N. Dahdah, A. Foudis, and D. Curnier. Multiparametric MRI as an indirect evaluation tool of the mechanical properties of in vitro cardiac tissues. *BMC Cardiovasc. Disord.* 13:24, 2013.

[54]Pfeffer, M. A., and E. Braunwald. Ventricular remodeling after myocardial infarction. Experimental observations and clinical implications. *Circulation* 81:1161–1172, 1990.

[55]Pfeffer, M. A., E. Braunwald, L. A. Moye, L. Basta, E. J. Brown, Jr, T. E. Cuddy, B. R. Davis, and E. M. Geltman. Effect of captopril on mortality and morbidity in patients with left ventricular dysfunction after myocardial infarction: results of the Survival and Ventricular Enlargement Trial. *N. Engl. J. Med.* 327:669–677, 1992.

[56]Pfeffer, M. A., J. M. Pfeffer, M. C. Fishbein, P. J. Fletcher, J. Spadaro, R. A. Kloner, and E. Braunwald. Myocardial infarct size and ventricular function in rats. *Circ. Res.* 44:503–512, 1979.

[57]Pilla, J. J., J. H. Gorman, and R. C. Gorman. Theoretic impact of infarct compliance on left ventricular function. *Ann. Thorac. Surg.* 87:803–810, 2009.

[58]Purcell, B. P., D. Lobb, M. B. Charati, S. M. Dorsey, R. J. Wade, K. N. Zellars, H. Doviak, S. Pettaway, C. B. Logdon, J. A. Shuman, P. D. Freels, J. H. Gorman, R. C. Gorman, F. G. Spinale, and J. A. Burdick. Injectable and bioresponsive hydrogels for on-demand matrix metalloproteinase inhibition. *Nat. Mater.* 13:653–661, 2014.

[59]Roberts, C. S., D. Maclean, P. Maroko, and R. A. Kloner. Early and late remodeling of the left ventricle after acute myocardial infarction. *Am. J. Cardiol.* 54:407–410, 1984.

[60]Ross, A. J., Z. Yang, S. S. Berr, W. D. Gilson, W. C. Petersen, J. N. Oshinski, and B. A. French. Serial MRI evaluation of cardiac structure and function in mice after reperfused myocardial infarction. *Magn. Reson. Med.* 47:1158–1168, 2002.

[61]Ryan, L. P., K. Matsuzaki, M. Noma, B. M. Jackson, T. J. Eperjesi, T. J. Plappert, M. G. S. John-Sutton, J. H. Gorman, III, and R. C. Gorman. Dermal filler injection: a novel approach for limiting infarct expansion. *Ann. Thorac. Surg.* 87:148–155, 2009.

[62]Sacks, M. S., and W. Sun. Multiaxial mechanical behavior of biological materials. *Annu. Rev. Biomed. Eng.* 5:251–284, 2003.

[63]Schmidt, A., C. F. Azevedo, A. Cheng, S. N. Gupta, D. A. Bluemke, T. K. Foo, G. Gerstenblith, R. G. Weiss, E. Marbán, G. F. Tomaselli, J. A. C. Lima, and K. C. Wu. Infarct tissue heterogeneity by magnetic resonance imaging identifies enhanced cardiac arrhythmia susceptibility in patients with left ventricular dysfunction. *Circulation* 115:2006–2014, 2007.

[64]Selvaraj, S., F. G. Aguilar, E. E. Martinez, L. Beussink, K.-Y. A. Kim, J. Peng, D. C. Lee, A. Patel, J. Sha, M. R. Irvin, D. K. Arnett, and S. J. Shah. Diastolic wall strain: a simple marker of abnormal cardiac mechanics. *Cardiovasc. Ultrasound* 12:40, 2014.

[65]Singelyn, J. M., P. Sundaramurthy, T. D. Johnson, P. J. Schup-Magoffin, D. P. Hu, D. M. Faulk, J. Wang, K. M. Mayle, K. Bartels, M. Salvatore, A. M. Kinsey, A. N. Demaria, N. Dib, and K. L. Christman. Catheter-deliverable hydrogel derived from decellularized ventricular extracellular matrix increases endogenous cardiomyocytes and preserves cardiac function post-myocardial infarction. *J. Am. Coll. Cardiol.* 59:751–763, 2012.

[66]Soleimanifard, S., K. Z. Abd-Elmoniem, T. Sasano, H. K. Agarwal, M. R. Abraham, T. P. Abraham, and J. L. Prince. Three-dimensional regional strain analysis in porcine myocardial infarction: a 3T magnetic resonance tagging study. *J. Cardiovasc. Magn. Reson.* 14:85, 2012.

[67]Spinale, F. G., M. L. Coker, S. R. Krombach, R. Mukherjee, H. Hallak, W. V. Houck, M. J. Clair, S. B. Kribbs, L. L. Johnson, J. T. Peterson, and M. R. Zile. Matrix metalloproteinase inhibition during the development of congestive heart failure: effects on left ventricular dimensions and function. *Circ. Res.* 85:364–376, 1999.

[68]Sun, Y., and K. T. Weber. Infarct scar: a dynamic tissue. *Cardiovasc. Res.* 46:250–256, 2000.

[69]Sutton, M. G., and N. Sharpe. Left ventricular remodeling after myocardial infarction: pathophysiology and therapy. *Circulation* 101:2981–2988, 2000.

[70]Takahashi, T., M. J. Levine, and W. Grossman. Regional diastolic mechanics of ischemic and nonischemic myocardium in the pig heart. *J. Am. Coll. Cardiol.* 17:1203–1212, 1991.

[71]Theroux, P., J. Ross, D. Franklin, J. W. Covell, C. M. Bloor, and S. Sasayama. Regional myocardial function and dimensions early and late after myocardial infarction in the unanesthetized dog. *Circ. Res.* 40:158–165, 1977.

[72]Thomopoulos, S., G. M. Fomovsky, and J. W. Holmes. The development of structural and mechanical anisotropy in fibroblast populated collagen gels. *J. Biomech. Eng.* 127:742, 2005.

[73]Thorstensen, A., B. H. Amundsen, H. Dalen, P. Hala, G. Kiss, S. A. Aase, H. Torp, and A. Støylen. Strain rate imaging combined with wall motion analysis gives incremental value in direct quantification of myocardial infarct size. *Eur. Heart J. Cardiovasc. Imaging* 13:914–921, 2012.

[74]Thygesen, K., *et al*. Third universal definition of myocardial infarction. *J. Am. Coll. Cardiol.* 60:1581–1598, 2012.

[75]Urheim, S., T. Edvardsen, K. Steine, H. Skulstad, E. Lyseggen, O. Rodevand, O. A. Smiseth, and A. Otto. Postsystolic shortening of ischemic myocardium: a mechanism of abnormal intraventricular filling. *Am. J. Physiol. Heart Circ. Physiol.* 284(6):H2343–H2350, 2003.

[76]Urheim, S., T. Edvardsen, H. Torp, B. Angelsen, and O. A. Smiseth. Myocardial strain by Doppler echocardiography:

validation of a new method to quantify regional myocardial function. *Circulation* 102:1158–1164, 2000.

[77]Weisman, H. F., D. E. Bush, J. A. Mannisi, and B. H. Bulkley. Global cardiac remodeling after acute myocardial infarction: a study in the rat model. *J. Am. Coll. Cardiol.* 5:1355–1362, 1985.

[78]Weisman, H. F., D. E. Bush, J. A. Mannisi, M. L. Weisfeldt, and B. Healy. Cellular mechanisms of myocardial infarct expansion. *Circulation* 78:186–201, 1988.

[79]Whittaker, P., D. R. Boughner, and R. A. Kloner. Role of collagen in acute myocardial infarct expansion. *Circulation* 84:2123–2134, 1991.

[80]Whittaker, P., R. A. Kloner, D. R. Boughner, and J. G. Pickering. Quantitative assessment of myocardial collagen with picrosirius red staining and circularly polarized light. *Basic Res. Cardiol.* 89(5):397–410, 1994.

[81]Yarbrough, W. M., R. Mukherjee, T. A. Brinsa, K. B. Dowdy, A. A. Scott, G. P. Escobar, C. Joffs, D. G. Lucas, F. A. Crawford, and F. G. Spinale. Matrix metalloproteinase inhibition modifies left ventricular remodeling after myocardial infarction in pigs. *J. Thorac. Cardiovasc. Surg.* 125:602–610, 2003.

[82]Yeon, S. B., N. Reichek, B. A. Tallant, J. A. Lima, L. P. Calhoun, N. R. Clark, E. A. Hoffman, K. K. Ho, and L. Axel. Validation of in vivo myocardial strain measurement by magnetic resonance tagging with sonomicrometry. *J. Am. Coll. Cardiol.* 38:555–561, 2001.

[83]Yin, F. C., R. K. Strumpf, P. H. Chew, and S. L. Zeger. Quantification of the mechanical properties of noncontracting canine myocardium under simultaneous biaxial loading. *J. Biomech.* 20(6):577–589, 1987.

[84]Zhang, Y., A. K. Y. Chan, C.-M. Yu, G. W. K. Yip, J. W. H. Fung, W. W. M. Lam, N. M. C. So, M. Wang, E. B. Wu, J. T. Wong, and J. E. Sanderson. Strain rate imaging differentiates transmural from non-transmural myocardial infarction: a validation study using delayed-enhancement magnetic resonance imaging. *J. Am. Coll. Cardiol.* 46:864–871, 2005.

[85]Zhang, Z., D. Dione, B. A. Lin, J. S. Duncan, A. J. Sinusas, and S. Sampath. Early diastolic function observed in canine model of reperfused transmural myocardial infarction using high temporal resolution MR imaging. *J. Cardiovasc. Magn. Reson.* 14:W65, 2012.

[86]Zimmerman, S. D., W. J. Karlon, J. W. Holmes, J. H. Omens, and J. W. Covell. Structural and mechanical factors influencing infarct scar collagen organization Structural and mechanical factors influencing infarct scar collagen organization. *Am. J. Physiol. Heart Circ. Physiol.* 278:H194–H200, 2000.